


**STUDY OF THE EFFECTS OF NANOPARTICLES CONTAINING A-HUMULENE
ON MEMORY ANALYSIS THROUGH BEHAVIORAL TESTS IN A B-AMYLOID 1-
42 NEUROINFLAMMATION MODEL**

**ESTUDO DOS EFEITOS DE NANOPARTÍCULAS CONTENDO A-HUMULENO
NA ANÁLISE DE MEMÓRIA ATRAVÉS DE TESTES COMPORTAMENTAIS EM
UM MODELO DE NEUROINFLAMAÇÃO B-AMILÓIDE 1-42**

**ESTUDIO DE LOS EFECTOS DE LAS NANOPARTÍCULAS QUE CONTIENEN
A-HUMULENO EN EL ANÁLISIS DE LA MEMORIA MEDIANTE PRUEBAS
CONDUCTUALES EN UN MODELO DE NEUROINFLAMACIÓN B-AMILOIDE 1-
42**

 <https://doi.org/10.56238/arev7n6-217>

Date of submission: 05/17/2025

Date of publication: 06/17/2025

**Laís Fernanda Dranski¹, Rafaela de Almeida Cardoso Goes², Angela Dubiela Julik³,
Eliane Gonçalves de Jesus Fonseca⁴, Ana Carolina Dorigoni Bini⁵, Patricia Tyski
Suckow⁶, Luciano Pavan Rossi⁷**

¹ Neuroanatomy and Neurophysiology Laboratory, Master in Nanosciences and Biosciences
Central-West State University (UNICENTRO)
E-mail: dranski@hotmail.com

ORCID: <https://orcid.org/0000-0003-4091-3544>
LATTES: <http://lattes.cnpq.br/5014605095768040>

² Neuroanatomy and Neurophysiology Laboratory, Undergraduate in Medicine
Central-West State University (UNICENTRO)
E-Mail: rafaelacardosogoess@gmail.com

ORCID: <https://orcid.org/0009-0006-8568-1678>
Lattes ID: <http://lattes.cnpq.br/7211474882603797>

³ PhD in Community Development
Central-West State University (Unicentro)
E-mail: adubiela@unicentro.br
ORCID: <https://orcid.org/0000-0001-7375-6771>
LATTES: <http://lattes.cnpq.br/6871512766056174>

⁴ PhD in Pharmaceutical Sciences
Central-West State University (Unicentro)
E-mail: egfonseca@unicentro.br
ORCID: <https://orcid.org/0009-0008-1160-0139>
LATTES: <http://lattes.cnpq.br/7714118092055404>

⁵ PhD in Pharmaceutical Sciences
Central-West State University (Unicentro)
E-mail: anacarolina@unicentro.br
ORCID: <https://orcid.org/0000-0003-1717-9249>
LATTES: <http://lattes.cnpq.br/0402666778625964>

⁶ PhD in Pharmaceutical Sciences
Central-West State University (Unicentro)
E-mail: patyski@unicentro.br
ORCID: <https://orcid.org/0000-0002-5022-7612>
LATTES: <http://lattes.cnpq.br/4474790121667662>

⁷ PhD in Performance Physiology
E-mail: lucianofisioo@yahoo.com.br
ORCID: <https://orcid.org/0000-0002-4271-5130>

ABSTRACT

The study investigated the effects of alpha-humulene, a sesquiterpene found in essential oils of plants such as Erva-baleeira, on behavior and memory in an experimental model of neuroinflammation induced by beta-amyloid peptide (1-42). Thirty-three *Rattus norvegicus* subjects were divided into four groups: negative control (CN), positive control (CP), treatment with alpha-humulene (HUM), and treatment with nanoparticles loaded with alpha-humulene (NHUM), with treatments administered for 15 days. The nanoparticles displayed specific characteristics (mean diameter: 210.1 ± 3.1 nm; polydispersity index: 0.090 ± 0.037 ; zeta potential: $+45.0 \pm 1.60$ mV; encapsulation efficiency: $+64.0 \pm 1.93\%$). In the Morris Water Maze test, the treatment groups showed significantly reduced latency times, indicating improved spatial memory. Moreover, in the conditioned fear test, the HUM and NHUM groups exhibited altered responses to visual and auditory stimuli compared to the control groups. In conclusion, nanoparticles containing alpha-humulene improved both behavioral outcomes and memory performance in this neuroinflammatory model, suggesting a potential therapeutic role in addressing deficits associated with beta-amyloid-induced neuroinflammation.

Keywords: Nanotechnology. Alpha-Humulene. Neuroinflammation.

RESUMO

O estudo investigou os efeitos do alfa-humuleno, um sesquiterpeno encontrado em óleos essenciais de plantas como a Erva-baleeira, sobre o comportamento e a memória em um modelo experimental de neuroinflamação induzida pelo peptídeo beta-amiloide (1-42). Trinta e três indivíduos da espécie *Rattus norvegicus* foram divididos em quatro grupos: controle negativo (CN), controle positivo (CP), tratamento com alfa-humuleno (HUM) e tratamento com nanopartículas carregadas com alfa-humuleno (NHUM), com tratamentos administrados por 15 dias. As nanopartículas apresentaram características específicas (diâmetro médio: $210,1 \pm 3,1$ nm; índice de polidispersão: $0,090 \pm 0,037$; potencial zeta: $+45,0 \pm 1,60$ mV; eficiência de encapsulamento: $+64,0 \pm 1,93\%$). No teste do Labirinto Aquático de Morris, os grupos de tratamento apresentaram tempos de latência significativamente reduzidos, indicando melhora da memória espacial. Além disso, no teste de medo condicionado, os grupos HUM e NHUM exibiram respostas alteradas a estímulos visuais e auditivos em comparação aos grupos controle. Em conclusão, nanopartículas contendo alfa-humuleno melhoraram tanto os resultados comportamentais quanto o desempenho da memória neste modelo neuroinflamatório, sugerindo um potencial papel terapêutico no tratamento de déficits associados à neuroinflamação induzida por beta-amiloide.

Palavras-chave: Nanotecnologia. Alfa-humuleno. Neuroinflamação.

LATTES: <http://lattes.cnpq.br/0942648139655127>

⁸ Professor of the Physiotherapy course at the State University of Central-UNICENTRO, Professor of the Master's program in Nanosciences and Biosciences - Unicentro. Professor of the Master's program in Veterinary Sciences - Unicentro. State University of Central-West (UNICENTRO)

E-mail: ikerppers@unicentro.br

ORCID: <https://orcid.org/0000-0002-5901-4007>

LATTES: <http://lattes.cnpq.br/2107257822885032>

RESUMEN

El estudio investigó los efectos del alfa-humuleno, un sesquiterpeno presente en aceites esenciales de plantas como la erva-baleeira, sobre el comportamiento y la memoria en un modelo experimental de neuroinflamación inducida por el péptido beta-amiloide (1-42). Treinta y tres sujetos de *Rattus norvegicus* se dividieron en cuatro grupos: control negativo (CN), control positivo (CP), tratamiento con alfa-humuleno (HUM) y tratamiento con nanopartículas cargadas con alfa-humuleno (NHUM), con tratamientos administrados durante 15 días. Las nanopartículas presentaron características específicas (diámetro medio: $210,1 \pm 3,1$ nm; índice de polidispersidad: $0,090 \pm 0,037$; potencial zeta: $+45,0 \pm 1,60$ mV; eficiencia de encapsulación: $+64,0 \pm 1,93\%$). En la prueba del Laberinto Acuático de Morris, los grupos de tratamiento mostraron tiempos de latencia significativamente reducidos, lo que indica una mejor memoria espacial. Además, en la prueba de miedo condicionado, los grupos HUM y NHUM mostraron respuestas alteradas a estímulos visuales y auditivos en comparación con los grupos control. En conclusión, las nanopartículas con alfa-humuleno mejoraron tanto los resultados conductuales como el rendimiento de la memoria en este modelo neuroinflamatorio, lo que sugiere un posible papel terapéutico para abordar los déficits asociados con la neuroinflamación inducida por beta-amiloide.

Palabras clave: Nanotecnología. Alfa-humuleno. Neuroinflamación.

INTRODUCTION

Experiences are fundamental keys for generating new memories and predisposing to learning. Based on behavioral observations regarding these two concepts, we can say that they directly interfere with our survival. They are responsible for creating memories and abilities, such as language, walking, recognizing people, names, emotions, avoiding danger, judgment, and even an individual's personality (Rabinovich et al., 2020; Bisaz et al., 2014).

For new learnings to occur, there are various processes involved: externally (in the environment) and the stimuli coming from it, as well as the individual's previous experiences. In the central nervous system (CNS), metabolic, biochemical, and structural factors come into play (McCarberg e Peppin, 2019; Herszage e Censor, 2018).

Thus, when there is an alteration in cerebral homeostasis, a series of gradual symptoms occur, with episodic memory loss that can lead to behavioral deterioration and impaired motor function, resulting in a permanent need for family care (Glaser et al., 2010).

There is evidence that the inflammatory mechanism is involved in the pathogenesis of many neuroprogressive diseases, resulting in irreversible brain damage (Troubat et al., 2021; Wyss, Coray and Mucke, 2002; Williams et al., 2022; Ozben and Ozben, 2019; Benedetti et al., 2020). Neuroinflammation is an immune response of the CNS that initially aims to eliminate harmful agents and metabolic waste, considered essential for brain protection. However, when mediated by innate brain immune cells, it becomes a chronic process, leading to functional changes and the death of neurons in the central or peripheral nervous system (Chagas et al., 2019; Lee et al., 2017; Facchinetti, Bronzuoli and Scuderi, 2018).

In this context, we can understand the complexity of the nervous system. One of the research strategies is to induce neuroinflammation in animal models to assess its effects, mechanisms, and resulting factors. The induction of inflammation can be carried out using different approaches. Fibrillary aggregates of the beta-amyloid protein ($A\beta$) are the main components of senile plaques found in the brain, closely related to accelerated neurodegeneration, impaired neuronal signaling, memory deficits, and the activation of transcription factors that induce a multitude of pro-inflammatory genes (Gremer et al., 2017; Belarbi et al., 2020; Brito et al., 2020; Simon, Tanner and Brundin, 2020; Uddin et al., 2020).

These findings are associated with diseases such as Alzheimer's disease, Parkinson's disease, Amyotrophic Lateral Sclerosis (ALS), among other neurodegenerative pathologies. Although pharmacological treatment is still limited for most neurodegenerative diseases, there has been a significant increase in research in recent years due to their high incidence and impact, leading to the development of new treatment approaches (Gitler, Dhillon and Shorter, 2017; Ransohoff, 2016; Scarpini, Galimberti and Ghezzi, 2013; Rodríguez and Herrera, 2014).

In light of the need for new approaches to the treatment of neuroinflammatory diseases, this study evaluated the response of neuroinflammation in brain tissue after the induction of A β 1-42 and proposed a therapeutic approach to analyze the potential effects of the α -Humulene molecule when associated with nanoparticles.

MATERIALS AND METHODS

SAMPLE CALCULATION

To determine the sample size for the research, the central limit theorem was used, which provides mathematical support for the concept that the mean of a random sample from a large population tends to be close to the population's mean. The margin of error is 10%, confidence level is 95%, and homogeneity is 99%. According to Equation 1:

$$\text{(Equation 1) } n = p(1-p) \frac{Z^2}{e^2}$$

Where: "n" is the sample size, "p" is the expected proportion, "Z" is the normal distribution value for a given confidence level, and "e" is the margin of error.

SAMPLE

This is an experimental, descriptive, and observational study conducted in the Neuroanatomy laboratory of the University of the West-Central State (UNICENTRO), with approval from the Institutional Animal Care and Use Committee (CEUA), Protocol No. 031/2019. Official Letter No. 019/2021– CEUA/UNICENTRO.

The sample consisted of 33 animals of the *Rattus norvegicus* breed, with a weight range of 300-350 g. These animals were obtained from the Animal Facilities of the State Universities of Londrina (UEL) and Maringá (UEM) in the state of Paraná.

Five animals were kept per cage, meaning that CP, HUM, NHUM had two cages for each group, except for CN. The cages were made of unbreakable and autoclavable acrylic and were placed on shelves, maintained in a room with a 12-hour light/dark cycle (lights on

from 7 am to 7 pm) at a temperature of $23 \pm 1^{\circ}\text{C}$, controlled by a 7000 BTU air conditioner, as shown in Figure 3.

EXPERIMENTAL GROUPS

The animals were divided into four groups:

- Negative Control Group (CN): Comprising 3 animals for tests involving predominantly normal tissues.
- Positive Control Group (CP): Containing 10 animals, these received the injection of Beta-Amyloid (1-42) responsible for neuroinflammation but did not receive any treatments. Material collection and euthanasia were performed on the sixtieth day after induction.
- Alpha-Humulene Treated Group (HUM): 10 animals that received the injection of Beta-Amyloid (1-42) responsible for neuroinflammation and were treated with 65 μg of Alpha-Humulene dissolved in 0.9% saline via gavage for 15 days. Material collection and euthanasia were performed on the sixtieth day after peptide induction.
- Alpha-Humulene Nanoparticles Treated Group (NHUM): Comprising 10 animals, these received the injection of Beta-Amyloid (1-42) responsible for neuroinflammation and were treated with nanoparticles containing Alpha-Humulene for 15 days. Material collection and euthanasia were performed on the sixtieth day after neuroinflammation.

PREPARATION OF NANOPARTICLES

The nanoparticles were obtained using the anti-solvent precipitation method, following the methodology previously described (Bi et al., 2017; Sun, Dai and Gao, 2017; Li et al., 2018; Mohammed et al., 2017) with modifications. In this technique, coacervation occurs between Zein and Chitosan. Initially, the original solvent was prepared by dissolving Zein in ethanol (87% v/v) with stirring (600 rpm) at room temperature (25°C) for 3 hours to obtain a clear liquid (20 mg/mL). Then, Chitosan was suspended in acetic acid (1% p/v) to create an anti-solvent stock solution.

Next, the amount of anti-solvent (1% p/v Chitosan solution in acetic acid) was solubilized in an amount of the original solvent (20 mg/mL Zein solution, 87% v/v ethanol) rapidly under stirring (1500 rpm) for 1 minute. The volumetric ratio of Zein to Chitosan was

also controlled (1:3, 1:6, and 1:9) according to the variables, with volumes determined by factorial planning (1:3 [2.5 mL:7.5 mL], 1:6 [1.25 mL:8.75 mL], 1:9 [1 mL: 9 mL]).

Afterward, the suspension was placed in a rotary evaporator. After evaporation, the obtained suspensions were centrifuged at 3000 g/15°C for 20 minutes, and the supernatant was stored for further analysis. The Alpha-Humulene nanoparticles were prepared in the same manner as described above. In detail, the amount used was 500 µL of Humulene for 2.5 mL of Zein (mixing ratio is 1:10), completely dissolved in the original solvent before mixing with the anti-solvent. The other experimental parameters remained constant.

NANOPARTICLE ANALYSIS AVERAGE DIAMETER (NM) AND POLYDISPERSITY INDEX (PDI)

The average diameter and polydispersity index (PDI) of Alpha-Humulene nanoparticles were determined using dynamic light scattering (DLS) (BIC 90 Plus, Brookhaven Instruments Corp., Holtsville, NY). For the analysis, an aliquot of nanoparticle suspensions was collected before the incubation with chitosan and after incubation for size and PDI comparison. The nanoparticles were dispersed in ultrapure water (1:200 v/v) and placed in a cuvette for analysis. All measurements were performed in triplicate, with a scattering angle of 90° at 25°C and a laser wavelength of 659 nm.

ZETA POTENTIAL (MV)

The Zeta potential of Alpha-Humulene nanoparticles was determined from the electrophoretic mobility of suspended nanoparticles. Samples were diluted (1:200 v/v) in a 1 mM KCl solution and placed in an electrophoretic cell at 25°C under a potential of ±150 mV (ZetaSizer ZS, Malvern, UK). The Zeta potential was analyzed before and after the incubation of nanoparticles with chitosan. Measurements were performed in triplicate and expressed as mean ± standard deviation.

ENCAPSULATION EFFICIENCY (EE)

To determine the amount of Alpha-Humulene encapsulated in nanoparticles, an indirect analysis was applied. An aliquot of the supernatant resulting from ultracentrifugation of the nanoparticles was diluted in the mobile phase, filtered through a 0.22 µm membrane, and analyzed by HPLC (Waters 2695-Alliance, Milford, USA). The analysis was performed in triplicate. The mobile phase consisted of Methanol, Phosphate Buffer pH 6.8, and

Acetonitrile (63:30:7 v/v/v) at a flow rate of 0.9 mL/min. The PDA detector was set to 306 nm. The percentage of EE was determined in at least three repetitions, as per Equation 2. The results were expressed as mean \pm standard deviation.

SURGICAL PROCEDURE

The animals were anesthetized with a solution in a proportion of 80 mg/kg of ketamine hydrochloride (ketamine, 10 mL bottle) to 15 mg/kg of xylazine hydrochloride (dopaser 10 mL bottle) via intraperitoneal injection. They were then placed in a stereotaxic apparatus (David Kopf, USA) where their heads were fixed by the temporal ridge and upper incisors, under coordinates AP= -3.0 mm, ML= 1.6 mm, -1.6 mm, and DV= 3.0 mm, using the bregma as a reference point. They received 4 μ L of Beta-Amyloid (1-42) peptide via Hamilton syringe in the CA1 hippocampal region for the senile plaque process (13).

After receiving the Beta-Amyloid (1-42) peptide (Sigma-Aldrich) via Hamilton syringe in the CA1 hippocampal region over 10 minutes (0.4 μ L/min), the animals rested for 30 days for the inflammatory processes of hippocampal neurons to occur.

Euthanasia was performed on one animal per group to check for the presence of plaques and neurofibrils in the hippocampus. Only after this verification were the animals from the groups treated with Alpha-Humulene particles, Alpha-Humulene Nanoparticles, etc.

POST-SURGICAL ANALGESIA

Post-surgical analgesia was provided using tramadol hydrochloride at a dose of 10 mg/kg, administered orally every 12 hours for 7 days (Kamerman, Koller and Loram, 2007).

TREATMENT

Alpha-Humulene was acquired from Sigma-Aldrich Brazil, with CAS number 6753-98-6, in a volume of 1 mL containing 2000 grams. The animals received 6.5 μ g of Alpha-Humulene orally (gavage) in 3.25 μ L and the same concentration of nanoparticles containing the substance, for a period of 15 days.

BEHAVIORAL TESTS SPATIAL MEMORY ANALYSIS: MORRIS WATER MAZE (LATER WATER MAZE - LWM)

Spatial learning and memory function were determined through a special version of the water maze. The test was described by Morris (Vorhees and Williams, 2006), in which its spatial version (also referred to as the "hidden platform") is based on universal ability. It involves using environmental cues to find a target, allowing for escape from an unpleasant situation, acting as positive reinforcement.

The experiment was conducted in a dedicated testing room with indirect lighting, no open windows, and no beams of light. The maze itself consists of a circular pool simulated by a sealed and waterproof blue water tank with a capacity of 1000 liters (Stackman et al., 2016).

The pool was conceptually divided into 4 identical imaginary quadrants. Two centimeters below the water's surface, hidden from the experimental subject's view, there is a 12 cm diameter escape platform. The water for the test intentionally had a cloudy appearance, and the platform's surface is abrasive to allow the animal to climb onto it once detected. The LWM was divided into quadrants by color, and a camera was suspended above the water tank for the experimenter's assessment. The animals were released randomly from one of the starting points, forcing the animal to navigate using spatial cues to find the platform, which remained fixed in the same location throughout the experiment.

Each animal was trained five times before the experimental surgery, after induction, and after the treatment period. In each attempt to find the center of the maze, the animal had a maximum of 5 minutes, and if it couldn't find it, it was guided to the path. The observed aspects included the escape latency (the time the animal took to reach the platform) and motor ability (how it swam) (Azmand and Rajaei, 2021).

AVERSIVE MEMORY

The rats were trained in the fear conditioning task. In this task, a training chamber was used (MED-VFC2-SCT-R model, Med Associates Inc., St. Albans, Vermont 05478), consisting of an aluminum box (35 x 35 x 35 cm) with a floor made of parallel stainless steel bars spaced 0.8 mm apart. This training box is placed within a larger box, acoustically isolated to reduce external sound interference.

According to Junior and Faria (Mourão Júnior and Faria, 2010), the study of the biological basis of learning and memory began with Ivan Pavlov in his treatise "Conditioned

reflexes: an integrated investigation of the physiological activity of the cerebral cortex" (Pavlov, 2010), which established the principles of associative conditioning, also known as classical conditioning or Pavlovian conditioning.

The animals were initially subjected to an individual training session in which they were carefully placed on the platform fixed in the center of the inhibitory avoidance box to explore it. When they descended from the platform with all four paws onto the steel bars of the box floor, they received the following stimuli: a 2-second sound and a 5-second light, creating a cycle (Scott et al., 2021).

The behavioral measure evaluated in this study was freezing time during the test sessions. This response was operationally defined by the absence of all bodily movements (except those involved in breathing) for a minimum of 6 seconds.

EUTHANASIA

The animals were anesthetized with 80 mg/kg of Ketamine and 15 mg/kg of Xylazine, and once their anesthetic state was confirmed, they received a lethal dose of 175 mg/kg of Pentobarbital intraperitoneally.

IMMUNOHISTOCHEMISTRY

The vials were lyophilized with 0.05 or 0.2 mL of deionized water. Antibody dilutions were made in buffer containing 1-3% bovine serum albumin. Antibodies for IL-1 and Anti β -Amyloid were used. For the immunohistochemistry (IHC) technique, slides were prepared as described for histological analysis, containing two sections per slide, per experimental group. Thermal deparaffinization was carried out for 16 hours in an oven at 60°C. Subsequently, chemical deparaffinization was performed with two immersion baths in Xylene for 10 minutes each and one immersion bath in 70° alcohol for another 10 minutes. After a water bath, the slides were immersed in a closed container in a Sodium Citrate solution and placed in a water bath for 30 minutes for antigen retrieval. Field marking was performed as described by Panis et al. (2011); the sections were outlined with a hydrophobic pen (Dako Pen®), and endogenous peroxidases were blocked with 10% hydrogen peroxide solution for 30 minutes, followed by non-specific binding blocking through incubation in 0.1% fetal serum for 1 hour. Subsequently, the sections were incubated with primary antibodies from Santa Cruz Anti Beta (1:300) and IL-1 (1:300) in a humid chamber overnight at 4°C for 2 hours. After incubation, the slides underwent three

rinses (5 minutes each) in phosphate-buffered saline (PBS). They were then incubated with secondary antibody and left for 15 minutes. The slides were again rinsed with PBS under a stream and had three more drops of PBS. Staining was revealed by incubation with 3,3'-diaminobenzidine for 15 minutes, followed by two PBS rinses, the first under a stream and the second as drops. In the final stage, the sections were lightly stained with Harry's hematoxylin (Merck) for 30 minutes and then rinsed with running water. They were incubated in 70° alcohol for 5 minutes in an immersion bath. Incubated in 95° alcohol for 5 minutes in an immersion bath. Incubated in Xylene for 5 minutes and incubated again in Xylene for 10 minutes. After draining all the liquid, the slides were mounted with Canadian balsam and a coverslip. Immunoreactions were performed with IL-1 and Anti-Beta Amyloid antibodies on the samples (a total of 33 samples). The selection of samples was based on morphological evaluation, giving preference to those with characteristic findings for each IHC. Their assessment was carried out following positivity standards. Negative controls were prepared in serial sections, and the intensity and location of immunoreactivity with all primary antibodies used were examined throughout the slide using an optical microscope. As a negative control, the primary antibody was omitted. For image analysis, colored photomicrographs of representative areas (400x magnification) were digitally acquired. For the semi-quantitative score, the images, a total of 10 images for each section of each animal, were evaluated using the color deconvolution tool of the Image J software (NIH, USA). Pixels were categorized as described previously by Chatterjee et al. (2013), as strong positive (3+), positive (2+), weak positive (1+), and negative (0).

STATISTICAL ANALYSIS

The obtained data were organized in spreadsheets and analyzed using Prism 9.0 software. For Gaussian analysis, the Shapiro-Wilk test was used. For non-parametric samples, the Kruskal-Wallis test with Dunn's post-test was employed.

RESULTS

NANOPARTICLES' SIZE

Among the results regarding the nanoparticles' size, it was possible to observe variations. This can occur due to various factors such as the formulation components (surfactant, drug characteristics) and production techniques (temperature, time, and equipment) (Souto, Severino and Santana, 2012). The Polydispersity Index (PDI) is used to

describe the width of the particle size distribution. Values considered ideal for a monodisperse system are zero, and less than 0.3 for polydisperse systems (Jawahar, Meyyanathan and Reddy, 2013). In the study of α -Humulene nanoparticles, the values found were 0.090 ± 0.037 , which means that the nanoparticle can be considered slightly polydisperse. Zeta potential is described as an important indicator used to predict and control the stability of colloidal suspensions and emulsions, among other applications. When it takes on high, negative, or positive values, it indicates a stable suspension since particle repulsion prevents aggregation (Franzol and Rezende, 2015).

Table 1 shows that the Zeta potential of the formulations varied from $+45.0 \pm 1.60$ mV. The percentage of encapsulation efficiency (%EE) was calculated using Equation 1, and the obtained value was $+64.0 \pm 1.93$.

Table 1. Each table should include a title/caption being explanatory in itself with respect to the details discussed in the table. The title should be in small case with the first letter in caps. A full stop should be placed at the end of the title.

Average diameter (nm)	IP	Zeta Potential (mV)	Encapsulation efficiency (%)
210.1 ± 3.1	$0,090 \pm 0,037$	$+45,0 \pm 1,60$	$+64,0 \pm 1,93$

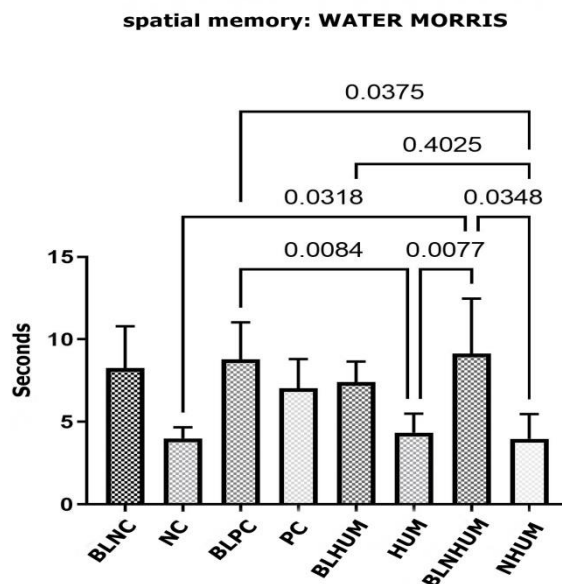
* Symbols and nonstandard abbreviations should be explained in the end of the text.

BEHAVIORAL ASSESSMENT

Morris Water Maze

The test applied is a standard task to evaluate learning and spatial memory acquisition abilities in animals dependent on the hippocampus (Lu et al., 2014). It measures the latency time for the animal to locate a submerged platform in a tank with turbid water [40]. Figure 1 presents the results of the animals' behavioral performance represented by Mean and Standard Deviation. Pre-induction is denoted as baseline (LB), LBCN 8.267 ± 2.527 s, LBCP 8.797 ± 2.236 s, LBHUM 7.41 ± 1.241 s, LBNHUM 9.144 ± 3.321 s. Post-treatment results were HUM 4.338 ± 1.15 s, NHUM 3.971 ± 1.497 s. The CN group had results of 3.99 ± 0.6785 s, and CP group 7.031 ± 1.78 s.

Fig. (1). Time in seconds for spatial memory - LBCN (negative control group baseline), CN (negative control group), CP (positive control group), LBHUM (HUM group baseline), HUM (HUM group), LBNHUM (Humulene nanoparticle group baseline).



Source: Author (2022).

It is noticeable that initially, all groups had similar average times. However, when analyzing the CP group, it is possible to observe that it remained with almost the same average after the induction of the peptide responsible for neuroinflammation, indicating impaired memory recall caused by the deposition of Beta-Amyloid 1-42.

In the HUM and NHUM groups, even though they did not yield significantly positive results when compared to the CP group, it is possible to identify that there were no major memory impairments in the animals. These groups can be compared with the CN group, which was not subjected to neuroinflammation induction.

The averages of the HUM and NHUM groups are similar, indicating that the molecule had the ability to mitigate the inflammatory process. However, when analyzing nanoparticles containing α -Humulene, there is a percentage-based trend indicating that their results were 4.0% higher than the HUM group, suggesting a positive trend for nanoparticle treatment to be more effective.

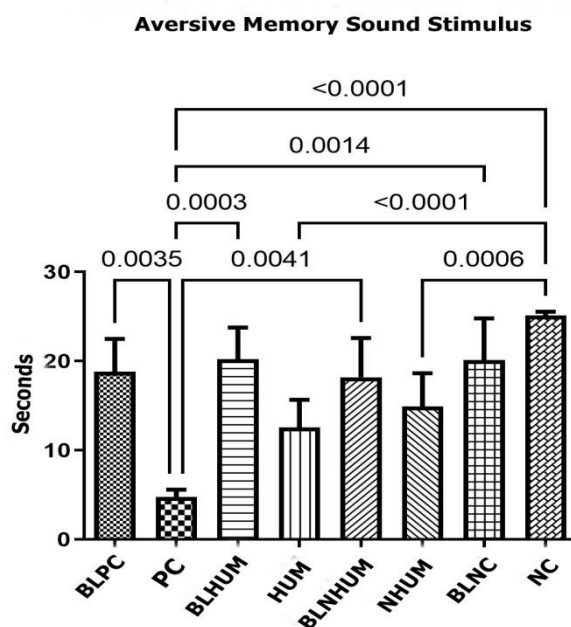
AVERSIVE MEMORY ASSESSMENT

Conditioned Fear Task In the evaluation of tests related to aversive stimuli, it is expected that animals exposed to neuroinflammation induction and treatment will show a longer latency time in freezing, which is recorded as an index of associative fear learning

and memory during the test. To create an aversive context, two stimuli were designated in addition to the box, as represented below.

Figure 2 presents the results of the Mean and Standard Deviation of the freezing time of animals in the Light stimulus. Pre-induction is denoted as the baseline (LB). LBCP $24.95 \pm 3.941s$, LBHUM $22.95 \pm 3.495s$, LBNHUM $24.74 \pm 2.421s$, LBCN $27.38 \pm 1.440s$. Post-treatment results: HUM $15.69 \pm 4.570s$, NHUM $17.74 \pm 4.781s$. And the control groups: CP $8.615 \pm 0.9547s$, CN $25.28 \pm 2.321s$.

Fig. (2). Aversive Memory Sound Stimulus - Mean seconds the animals remained in freezing. - LBCP (baseline of the positive control group), CP (positive control group), LBHUM (baseline of the HUM group), HUM (HUM group), LBNHUM (baseline of the Humulene nanoparticle group). *The data values expressed represent in seconds the time it took for the animals to find the platform.



Source: Author (2022).

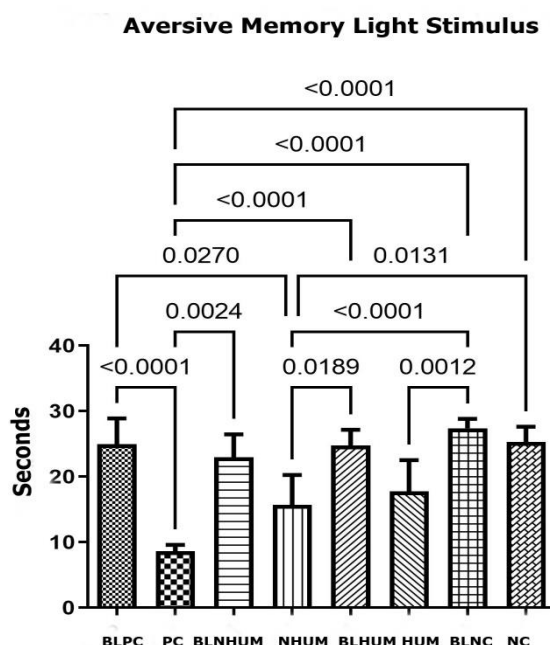
When comparing the groups, it is noticeable that all groups had similar initial averages at the baselines. After the induction of the peptide, the freezing time averages of the CP group showed a significant reduction in the maintenance of learning. According to the graph, it is possible to verify that neuroinflammation was responsible for the decreased maintenance of learning, meaning the recall of aversive memory in response to the light stimulus.

However, the groups of animals that received the proposed treatments in the protocol obtained better results in maintaining learning - HUM and NHUM. Even without a statistically significant difference, it is evident that the averages of the animals treated with

nanoparticles containing α -Humulene outperformed the group treated with the isolated molecule.

Figure 3 shows the Mean and Standard Deviation results of the freezing time of animals in the Sound stimulus. Baseline (LB). LBCP $18.82 \pm 3.652s$, LBHUM $20.21 \pm 3.558s$, LBNHUM $18.19 \pm 4.399s$, LBCN $20.11 \pm 4.666s$. Post-treatment results: HUM $4.763 \pm 0.8291s$, NHUM $14.92 \pm 3.730s$. Control Groups: CP $4.763 \pm 0.8291s$, CN $25.12 \pm 0.4272s$.

Fig. (3). Aversive Memory Light Stimulus. Mean seconds the animals remained in freezing. LBCP (baseline of the positive control group), CP (positive control group), LBHUM (baseline of the HUM group), HUM (HUM group), LBNHUM (baseline of the Humulene nanoparticle group). *The data values expressed represent in seconds the time it took for the animals to find the platform.



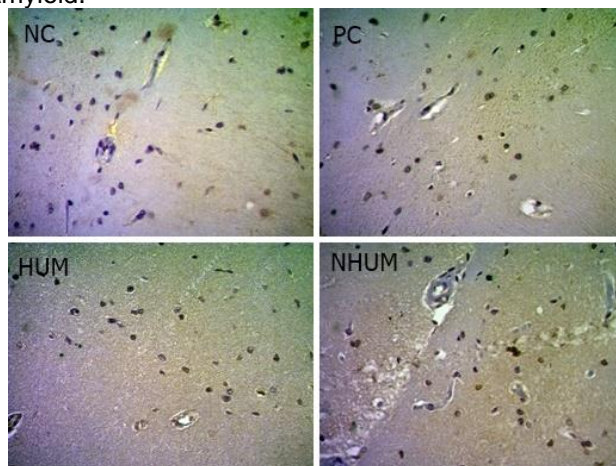
Source: Author (2022)

When faced with the sound stimulus, it is possible to notice that the initial averages are also similar, and as described earlier, the animals had a reduction in the maintenance of aversive memory after the peptide induction. The group that received only the peptide induction without treatment, denoted as CP, had a statistically significant decrease in memory maintenance compared to the treated groups, HUM and NHUM. Just like the other results, for the groups treated with nanoparticles (NHUM), it is evident that the freezing time average was higher than that of the HUM group.

IMMUNOHISTOCHEMISTRY ANALYSIS

Immunohistochemistry Analysis of the expression of inflammatory cytokines IL-1 in the hippocampal CA1 region, as shown in Figure 4.

Fig. (4). Immunohistochemical reaction of IL-1. CP (positive control), CN (negative control), HUM (Humulene), and NHUM (Humulene Nanoparticle), all at 400x magnification. The arrows in the figures indicate areas where there is deposition of Beta-Amyloid.

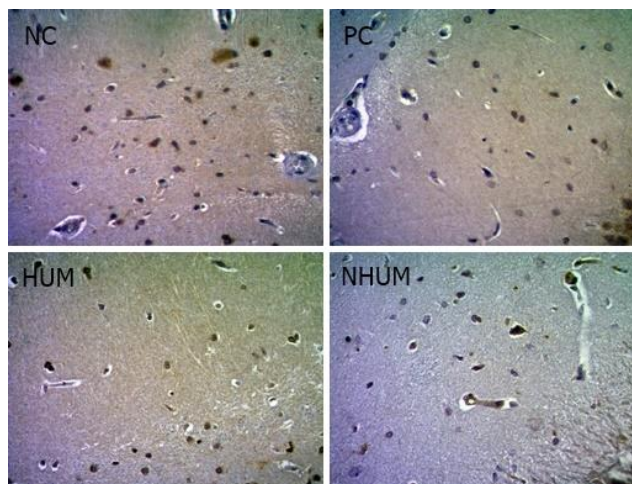


Source: Author (2022).

To confirm the inflammatory effect after the induction of A β 1-42, immunohistochemical analyses were conducted, revealing the expression of IL-1 cytokines, as previously described, through strong positive staining. The intensity of antibody labeling for inflammation in the CP groups confirms that the neuroinflammatory process is occurring in the CA1 area under study since interleukins, such as IL-1, serve as immune response mediators.

In the treated groups referred to as HUM and NHUM, it can be observed that treatment with the α -Humulene molecule and α -Humulene nanoparticles led to a significant reduction in cytokine expression, attenuating signs of inflammation, which can be categorized as weak positive, comparable to the CN group, classified as negative.

Fig. (5). Anti- β -Amyloid Immunohistochemical Reaction in CP (positive control), HUM (Humulene), and NHUM (Humulene Nanoparticle), all at 400x magnification. The arrows in the figures indicate areas with Beta-Amyloid deposition.



Source: Author (2022).

DISCUSSION

Understanding how certain pathologies affect the central nervous system (CNS) is crucial for identifying the brain structures most affected, leading to irreversible changes. Therefore, it is essential to explore new strategies to promote and restore an individual's health.

According to Stephenson et al. (2018), neurodegenerative diseases have emerged as the leading cause of morbidity and disability, with a significant socio-economic impact. The increasing incidence of these diseases has been growing exponentially with the aging population, affecting 50-70% of this demographic (Charchat, Fichman et al., 2005; Trevisan et al., 2019; Tromp et al., 2015). Although they are considered highly relevant, the etiology of these diseases is still not precise, with hypotheses including infections, genetic mutations, traumas, protein aggregations, and chronic activation of an innate immune response in the CNS (Fekonja, Avbelj and Jerala, 2012; Glass et al., 2010; Golia et al., 2019; Naveh, Benjamin et al., 2007; Okun et al., 2009).

Pimentel (2018) suggests that the need to develop new treatment methods has led to a significant focus on nanotechnology. Nanoparticles are being used in various fields. In the production of medication, the benefits include a high surface-to-volume ratio, providing more contact surface to absorb and transport small biomolecules like DNA, RNA, drugs, proteins, and other molecules to the target site, thereby increasing the efficacy of therapeutic agents (Chaturvedi et al., 2019; Herdiana et al., 2021; Kumari, Luqman and

Meena, 2019; Muhamad, Plengsuriyakarn and Bangchang, 2018; Safari and Zarnegar, 2014; Yan et al., 2010).

Clementino et al. (2021) noted that hybrid nanoparticles composed of natural polysaccharides and phospholipids are efficient for drug delivery through various administration routes. In their studies, they obtained relatively small particle sizes (234.2 ± 8.8 nm) with a particle size distribution (IDP) of 0.094 ± 0.009 . Similarly, in the present study, the method of preparation involves hybrid particles, with nanoparticle sizes of 210.1 nm and an IDP of 0.090 ± 0.037 . According to the authors' considerations about the preparation, size, and IDP, it can be concluded that α -Humulene nanoparticles were efficient carriers for delivering the compound to the brain.

Another material used in the preparation of α -Humulene nanoparticles was Zein, a prolamina recommended for stable drug delivery systems. According to Marini et al. (2014), this prolamina is known to be non-reactive with other materials and can be obtained at a low cost as it is easily manufactured. It has a structure with more hydrophobic amino acids than hydrophilic ones, making it insoluble in water, a condition necessary for water-based formulations.

Regarding the Zeta potential properties, the results obtained were $0.090 \pm 1.60 \pm 45.0$, which, according to the findings in the study by Li et al. (2017), a value greater than 30 mV is considered stable. In other words, the nanoparticles in this study indicate high stability because a higher Zeta potential indicates that the particles are more likely to repel each other due to strong electrostatic repulsion within the suspension.

Basting et al. (2019) mentioned the advantages of using phytotherapeutic compounds as anti-inflammatories in experimental models of inflammation. They evaluated the effects on paw edema in male rats induced by carrageenan. The study author used a compound with high concentrations of α -Humulene and observed significant reductions in animal lesions.

According to authors Neto, Tamelini, and Forlenza (2005), most brain impairments initially manifest as dementia, followed by cognitive decline and deficits in visuospatial memory. These findings are associated with areas of greater damage. For example, in Alzheimer's disease (AD), the initial target is the pyramidal cells of the entorhinal cortex and their connections with the CA1 region of the hippocampus (MacDonald and Tonegawa, 2021).

In the present study, after the induction of the A β peptide in the CA1 region, behavioral memory and learning parameters were assessed. Following the studies by Hartley et al. (2014), the hippocampus (HPC) plays a crucial role in our reactions to the environment, such as mood, learning, memory, spatial balance, and the ability to remember events in their context.

Through the Morris Water Maze test (adapted), it is evident that there was initially a decrease in the time it took for the animals to find the platform. In other words, the animals were able to acquire relevant information to complete the task and maintain this memory during the test days. However, in the CP group, which received only induction of neuroinflammation without treatment, they had a longer latency time to complete the test and find the platform, indicating that they had memory and learning impairments due to the deposition of β -amyloid(1-42). This can be associated with the findings of Fan et al. (2015), which suggest that continuous neuroinflammation leads to the activation of immune response receptors, microglia activation, reduced phagocytic microglia, and subsequent neuronal damage and synaptic loss. This can be related to the inactivation of circuits, resulting in changes in neural connectivity that, in response to external stimuli, lead to impairments in long-term memory-related behavior.

In the HUM and NHUM groups, it is evident that the animals maintained similar time averages to the CN group. It is noticeable that the nanoparticles show a positive trend superior to the free compound. This can be explained by the high bioavailability and biodistribution and other characteristics of the nanoparticles that facilitate their passage through the blood-brain barrier (Silva, 2010).

Fidelis et al. (2019) compared nanoparticles containing curcumin with isolated curcumin compounds. The nanoparticles containing curcumin enhanced antioxidant effects. The justification is that the isolated compound has low bioavailability and biodistribution, and when assigned to nanoparticles with coated biodegradable polymers that can cross the intact blood-brain barrier, they reach optimal therapeutic concentrations in the brain, corroborating the findings of the present study.

Another method used for memory analysis was the fear conditioning task. According to Kim, Cho (2020), exposure to an aversive context activates a subset of regions in the medial temporal lobe cortex, including the hippocampal areas, neurons that transmit impulses directly to the amygdala, and other structures, resulting in memory formation. Repeating that context strengthens the hippocampal pathway, leading to learning and

memory retrieval (Barroca et al., 2019; Izquierdo, Furini and Myskiw, 2016; Jin and Maren, 2015; Yavas, Gonzalez and Fanselow, 2019; Schafe et al., 1999).

It is known that neural circuits of learning do not act in a singular and isolated manner but rather recruit different underlying neural systems in the brain during memory acquisition (Barsegyan et al., 2010). The conditioned fear stimulus context corresponds to explicit memory, subjecting animals to two stimuli (context, light, sound), and we have distinct neural information processing pathways. Consequently, the freezing time result averages can confirm this assertion.

With a brief analysis of the stimuli, it is possible to see that the average freezing time for the light stimulus was higher, indicating that this stimulus had a greater impact on the animals. Compared to the findings of Dias; Silva (2012), this fact can be justified based on neuroanatomy. The induction of neuroinflammation in the CA1 region affects the processing of auditory information corresponding to the sound stimulus. This aligns with our findings.

When comparing the CN group with the HUM and NHUM groups, it is evident that animals receiving nanoparticles show a positive trend towards an anti-inflammatory effect, attenuating long-term memory impairments. They had a higher average freezing time than the CN group in both stimuli.

In addition to behavioral tests, immunohistochemical analysis proved essential for a better understanding of the results. Through these tests, it was possible to identify cognitive impairments related to memory and learning induced 30 days after a single injection of the A β 1-42 peptide. Changes were observed in the glutamatergic system, altering levels of inflammatory interleukins, as shown by the IHC images.

According to Machado et al. (2020), the excessive accumulation of A β leads to the formation of plaques or tangles, which triggers immune system activation, setting off a cascade reaction involving the production of interleukins, macrophages, natural killer (NK) cells, B cells, T cells, and the release of immunoglobulins. This illustrates the elevated levels of pro-inflammatory cytokines as a hallmark of neurodegenerative disorders, in line with the current research.

Salim; Xavier (2014) noted that *Cordia verbenacea* has high concentrations of α -Humulene, which characterizes its anti-inflammatory properties. The compound was used in different inflammatory models, and afterward, levels of inflammatory cytokines and the expression of pro-inflammatory proteins were analyzed.

Abozaid et al. (2022) evaluated the role of resveratrol nanoparticles (used as antioxidants) in neurochemical and histopathological approaches in AD rats over 60 days. The authors described the effects of nanoparticles on cholinergic deficits, linked to A β clearance. They also noted that they regulated the levels of interleukin-1 (IL-1), reducing neuroinflammation in AD. Similar to the present study, it was possible to observe a reduction in the inflammatory process after treatment based on the regulation of antibodies and interleukins.

A review conducted by Duskey; Kreuter (2020) discussed the expected effects of nanoparticles and compared them with conventional drugs. The results analyzed confirmed greater efficiency of nanoparticles as they promoted better blood-brain barrier (BBB) penetration. This was attributed to their size, physicochemical properties, and material distribution, suggesting their promising use in treating brain diseases. The findings by Duskey; Kreuter (2020) align with the current research. α -Humulene nanoparticles have shown potential as anti-inflammatory therapeutic agents.

CONCLUSIONS

In the present study, it was possible to observe the behavioral effects of neuroinflammation on memory and learning, both initially (immediately after peptide induction) and subsequently, in relation to the therapeutic interventions proposed.

According to the results obtained, it is worth highlighting that there was a reduction in the neuroinflammatory process, attenuating impairments in both short-term and long-term memory. The therapeutic effectiveness hypothesis can be attributed to the characteristics of polymeric nanoparticles that cross the blood-brain barrier, reaching optimal concentrations in the central nervous system (CNS).

Therefore, it can be concluded that α -Humulene nanoparticles are capable of bringing improvements in behavioral and memory conditions. By combining a therapeutic agent with nanotechnology, we underscore the advancement of science, technology, and healthcare.

REFERENCES

1. RABINOVICH ORLANDI, I. et al. Behavioral tagging underlies memory reconsolidation. *Proceedings of the National Academy of Sciences*, v. 117, n. 30, p. 18029–18036, 28 jul. 2020.
2. BISAZ, R.; TRAVAGLIA, A.; ALBERINI, C. M. The neurobiological bases of memory formation: from physiological conditions to psychopathology. *Psychopathology*, v. 47, n. 6, p. 347–356, 2014.
3. MCCARBERG, B.; PEPPIN, J. Pain pathways and nervous system plasticity: learning and memory in pain. *Pain Medicine*, v. 20, n. 12, p. 2421–2437, 1 dez. 2019.
4. HERSZAGE, J.; CENSOR, N. Modulation of learning and memory: a shared framework for interference and generalization. *Neuroscience*, v. 392, p. 270–280, nov. 2018.
5. GLASER, V. et al. The intra-hippocampal leucine administration impairs memory consolidation and LTP generation in rats. *Cellular and Molecular Neurobiology*, v. 30, n. 7, p. 1067–1075, 26 out. 2010.
6. TROUBAT, R. et al. Neuroinflammation and depression: a review. *European Journal of Neuroscience*, v. 53, n. 1, p. 151–171, 20 jan. 2021.
7. WYSS-CORAY, T.; MUCKE, L. Inflammation in neurodegenerative disease—A double-edged sword. *Neuron*, v. 35, n. 3, p. 419–432, ago. 2002.
8. WILLIAMS, J. A. et al. Inflammation and brain structure in schizophrenia and other neuropsychiatric disorders. *JAMA Psychiatry*, v. 79, n. 5, p. 498, 1 maio 2022.
9. OZBEN, T.; OZBEN, S. Neuroinflammation and anti-inflammatory treatment options for Alzheimer's disease. *Clinical Biochemistry*, v. 72, p. 87–89, out. 2019.
10. BENEDETTI, F. et al. Neuroinflammation in bipolar depression. *Frontiers in Psychiatry*, v. 11, 26 fev. 2020.
11. CHAGAS, L. da S. et al. Rapid plasticity of intact axons following a lesion to the visual pathways during early brain development is triggered by microglial activation. *Experimental Neurology*, v. 311, p. 148–161, jan. 2019.
12. LEE, S. J. C. et al. Towards an understanding of amyloid- β oligomers: characterization, toxicity mechanisms, and inhibitors. *Chemical Society Reviews*, v. 46, n. 2, p. 310–323, 2017.
13. FACCHINETTI, R.; BRONZUOLI, M. R.; SCUDERI, C. An animal model of Alzheimer disease based on the intrahippocampal injection of amyloid β -peptide (1–42). In: *Protocols for Cell Death in Different Models*. 2018. p. 343–352.

14. GITLER, A. D.; DHILLON, P.; SHORTER, J. Neurodegenerative disease: models, mechanisms, and a new hope. *Disease Models & Mechanisms*, v. 10, n. 5, p. 499–502, 1 maio 2017.
15. RANSOHOFF, R. M. How neuroinflammation contributes to neurodegeneration. *Science*, v. 353, n. 6301, p. 777–783, 19 ago. 2016.
16. GREMER, L. et al. Fibril structure of amyloid- β (1–42) by cryo-electron microscopy. *Science*, v. 358, n. 6359, p. 116–119, 6 out. 2017.
17. BELARBI, K. et al. Glycosphingolipids and neuroinflammation in Parkinson's disease. *Molecular Neurodegeneration*, v. 15, n. 1, p. 59, 17 dez. 2020.
18. BRITO, D. V. C. et al. Mimicking age-associated Gadd45 γ dysregulation results in memory impairments in young adult mice. *The Journal of Neuroscience*, v. 40, n. 6, p. 1197–1210, 5 fev. 2020.
19. SIMON, D. K.; TANNER, C. M.; BRUNDIN, P. Parkinson disease epidemiology, pathology, genetics, and pathophysiology. *Clinics in Geriatric Medicine*, v. 36, n. 1, p. 1–12, fev. 2020.
20. UDDIN, M. S. et al. Revisiting the amyloid cascade hypothesis: from anti-A β therapeutics to auspicious new ways for Alzheimer's disease. *International Journal of Molecular Sciences*, v. 21, n. 16, p. 5858, 14 ago. 2020.
21. SCARPINI, E.; GALIMBERTI, D.; GHEZZI, L. Disease-modifying drugs in Alzheimer's disease. *Drug Design, Development and Therapy*, v. 7, p. 1471–1478, dez. 2013.
22. RODRÍGUEZ, J. L.; HERRERA, R. F. G. Demencias y enfermedad de Alzheimer en América Latina y el Caribe. *Revista Cubana de Salud Pública*, v. 40, n. 3, p. 378–387, 2014.
23. BI, C. et al. Particle size effect of curcumin nanosuspensions on cytotoxicity, cellular internalization, in vivo pharmacokinetics and biodistribution. *Nanomedicine*, v. 13, n. 3, p. 943–953, abr. 2017.
24. SUN, C.; DAI, L.; GAO, Y. Interaction and formation mechanism of binary complex between zein and propylene glycol alginate. *Carbohydrate Polymers*, v. 157, p. 1638–1649, fev. 2017.
25. LI, M. F. et al. The formation of zein–chitosan complex coacervated particles: relationship to encapsulation and controlled release properties. *International Journal of Biological Macromolecules*, v. 116, p. 1232–1239, set. 2018.
26. MOHAMMED, M. et al. An overview of chitosan nanoparticles and its application in non-parenteral drug delivery. *Pharmaceutics*, v. 9, n. 4, p. 53, 20 nov. 2017.
27. KAMERMAN, P.; KOLLER, A.; LORAM, L. Postoperative administration of the analgesic tramadol, but not the selective cyclooxygenase-2 inhibitor parecoxib, abolishes

- postoperative hyperalgesia in a new model of postoperative pain in rats. *Pharmacology*, v. 80, n. 4, p. 244–248, 2007.
28. VORHEES, C. V.; WILLIAMS, M. T. Morris water maze: procedures for assessing spatial and related forms of learning and memory. *Nature Protocols*, v. 1, n. 2, p. 848–858, 27 ago. 2006.
 29. STACKMAN, R. W. et al. Temporary inactivation reveals that the CA1 region of the mouse dorsal hippocampus plays an equivalent role in the retrieval of long-term object memory and spatial memory. *Neurobiology of Learning and Memory*, v. 133, p. 118–128, set. 2016.
 30. AZMAND, M. J.; RAJAEI, Z. Effects of crocin on spatial or aversive learning and memory impairments induced by lipopolysaccharide in rats. *Avicenna Journal of Phytomedicine*, v. 11, n. 1, p. 79–90, 2021.
 31. MOURÃO JÚNIOR, C. A.; FARIA, N. C. Memória. *Psicologia: Reflexão e Crítica*, v. 28, n. 4, p. 780–788, dez. 2015.
 32. PAVLOV, I. P. Conditioned reflexes: an investigation of the physiological activity of the cerebral cortex. *Annals of Neurosciences*, v. 17, n. 3, 1 jun. 2010.
 33. SCOTT, G. A. et al. Adult neurogenesis mediates forgetting of multiple types of memory in the rat. *Molecular Brain*, v. 14, n. 1, p. 97, 26 dez. 2021.
 34. PANIS, C. et al. Trypanosoma cruzi: effect of the absence of 5-lipoxygenase (5-LO)-derived leukotrienes on levels of cytokines, nitric oxide and iNOS expression in cardiac tissue in the acute phase of infection in mice. *Experimental Parasitology*, v. 127, n. 1, p. 58–65, jan. 2011.
 35. CHATTERJEE, S. et al. A novel activator of CBP/p300 acetyltransferases promotes neurogenesis and extends memory duration in adult mice. *Journal of Neuroscience*, v. 33, n. 26, p. 10698–10712, 26 jun. 2013.
 36. SOUTO, E. B.; SEVERINO, P.; SANTANA, M. H. A. Preparação de nanopartículas poliméricas a partir de polímeros pré-formados: parte II. *Polímeros*, v. 22, n. 1, p. 101–106, 27 jan. 2012.
 37. JAWAHAR, N. et al. Solid lipid nanoparticles for oral delivery of poorly soluble drugs. *ChemInform*, v. 44, n. 27, 2 jul. 2013.
 38. FRANZOL, A.; REZENDE, M. C. Estabilidade de emulsões: um estudo de caso envolvendo emulsionantes aniônico, catiônico e não-iônico. *Polímeros*, v. 25, esp., p. 1–9, dez. 2015.
 39. LU, C. L. et al. Taurine improves the spatial learning and memory ability impaired by sub-chronic manganese exposure. *Journal of Biomedical Science*, v. 21, n. 1, p. 51, 24 dez. 2014.

40. BERAKI, S. et al. Effects of repeated treatment of phencyclidine on cognition and gene expression in C57BL/6 mice. *International Journal of Neuropsychopharmacology*, v. 12, n. 2, p. 243, 7 mar. 2009.
41. STEPHENSON, J. et al. Inflammation in CNS neurodegenerative diseases. *Immunology*, v. 154, n. 2, p. 204–219, 17 jun. 2018.
42. CHARCHAT-FICHMAN, H. et al. Declínio da capacidade cognitiva durante o envelhecimento. *Revista Brasileira de Psiquiatria*, v. 27, n. 1, p. 79–82, mar. 2005.
43. TREVISAN, K. et al. Theories of aging and the prevalence of Alzheimer's disease. *BioMed Research International*, v. 2019, p. 1–9, 16 jun. 2019.
44. TROMP, D. et al. Episodic memory in normal aging and Alzheimer disease: insights from imaging and behavioral studies. *Ageing Research Reviews*, v. 24, p. 232–262, nov. 2015.
45. FEKONJA, O.; AVBELJ, M.; JERALA, R. Suppression of TLR signaling by targeting TIR domain-containing proteins. *Current Protein & Peptide Science*, v. 13, n. 8, p. 776–788, dez. 2012.
46. GLASS, C. K. et al. Mechanisms underlying inflammation in neurodegeneration. *Cell*, v. 140, n. 6, p. 918–934, mar. 2010.
47. GOLIA, M. T. et al. Interplay between inflammation and neural plasticity: both immune activation and suppression impair LTP and BDNF expression. *Brain, Behavior, and Immunity*, v. 81, p. 484–494, out. 2019.
48. NAVEH-BENJAMIN, M. et al. Age-related differences in immediate serial recall: dissociating chunk formation and capacity. *Memory & Cognition*, v. 35, n. 4, p. 724–737, jun. 2007.
49. OKUN, E. et al. Toll-like receptors in neurodegeneration. *Brain Research Reviews*, v. 59, n. 2, p. 278–292, mar. 2009.
50. PIMENTEL, L. F. et al. Nanotecnologia farmacêutica aplicada ao tratamento da malária. *Revista Brasileira de Ciências Farmacêuticas*, v. 43, n. 4, p. 503–514, dez. 2007.
51. CHATURVEDI, V. K. et al. Cancer nanotechnology: a new revolution for cancer diagnosis and therapy. *Current Drug Metabolism*, v. 20, n. 6, p. 416–429, 17 jul. 2019.
52. HERDIANA, Y. et al. Chitosan-based nanoparticles of targeted drug delivery system in breast cancer treatment. *Polymers (Basel)*, v. 13, n. 11, p. 1717, 24 maio 2021.
53. KUMARI, P.; LUQMAN, S.; MEENA, A. Application of the combinatorial approaches of medicinal and aromatic plants with nanotechnology and its impacts on healthcare. *DARU Journal of Pharmaceutical Sciences*, v. 27, n. 1, p. 475–489, 25 jun. 2019.

54. MUHAMAD, N.; PLENGSURIYAKARN, T.; NA-BANGCHANG, K. Application of active targeting nanoparticle delivery system for chemotherapeutic drugs and traditional/herbal medicines in cancer therapy: a systematic review. *International Journal of Nanomedicine*, v. 13, p. 3921–3935, jul. 2018.
55. SAFARI, J.; ZARNEGAR, Z. Advanced drug delivery systems: nanotechnology of health design – a review. *Journal of Saudi Chemical Society*, v. 18, n. 2, p. 85–99, abr. 2014.
56. YAN, F. et al. The effect of poloxamer 188 on nanoparticle morphology, size, cancer cell uptake, and cytotoxicity. *Nanomedicine*, v. 6, n. 1, p. 170–178, fev. 2010.
57. CLEMENTINO, A. et al. Hybrid nanoparticles as a novel tool for regulating psychosine-induced neuroinflammation and demyelination *in vitro* and *ex vivo*. *Neurotherapeutics*, v. 18, n. 4, p. 2608–2622, 3 out. 2021.
58. MARINI, V. G. et al. Biodegradable nanoparticles obtained from zein as a drug delivery system for terpinen-4-ol. *Química Nova*, 2014.
59. BASTING, R. T. et al. *Pterodon pubescens* and *Cordia verbenacea* association promotes a synergistic response in antinociceptive model and improves the anti-inflammatory results in animal models. *Biomedicine & Pharmacotherapy*, v. 112, p. 108693, abr. 2019.
60. GALLUCCI NETO, J.; TAMELINI, M. G.; FORLENZA, O. V. Diagnóstico diferencial das demências. *Archives of Clinical Psychiatry (São Paulo)*, v. 32, n. 3, p. 119–130, jun. 2005.
61. MACDONALD, C. J.; TONEGAWA, S. Crucial role for CA2 inputs in the sequential organization of CA1 time cells supporting memory. *Proceedings of the National Academy of Sciences*, v. 118, n. 3, 19 jan. 2021.
62. HARTLEY, T. et al. Space in the brain: how the hippocampal formation supports spatial cognition. *Philosophical Transactions of the Royal Society B: Biological Sciences*, v. 369, n. 1635, p. 20120510, 5 fev. 2014.
63. FAN, K. et al. The induction of neuronal death by up-regulated microglial cathepsin H in LPS-induced neuroinflammation. *Journal of Neuroinflammation*, v. 12, n. 1, p. 54, 19 dez. 2015.
64. SILVA, G. A. Nanotechnology applications and approaches for neuroregeneration and drug delivery to the central nervous system. *Annals of the New York Academy of Sciences*, v. 1199, n. 1, p. 221–230, 17 jun. 2010.
65. FIDELIS, E. M. et al. Curcumin-loaded nanocapsules reverses the depressant-like behavior and oxidative stress induced by β -amyloid in mice. *Neuroscience*, v. 423, p. 122–130, dez. 2019.
66. KIM, W. B.; CHO, J. H. Encoding of contextual fear memory in hippocampal–amygdala circuit. *Nature Communications*, v. 11, n. 1, p. 1382, 13 mar. 2020.

67. BARROCA, N. C. B. et al. Influence of aversive stimulation on haloperidol-induced catalepsy in rats. *Behavioural Pharmacology*, v. 30, n. 2–3, p. 229–238, abr. 2019.
68. IZQUIERDO, I.; FURINI, C. R. G.; MYSKIW, J. C. Fear memory. *Physiological Reviews*, v. 96, n. 2, p. 695–750, abr. 2016.
69. JIN, J.; MAREN, S. Prefrontal-hippocampal interactions in memory and emotion. *Frontiers in Systems Neuroscience*, v. 9, 15 dez. 2015.
70. YAVAS, E.; GONZALEZ, S.; FANSELOW, M. S. Interactions between the hippocampus, prefrontal cortex, and amygdala support complex learning and memory. *F1000Research*, v. 8, p. 1292, 31 jul. 2019.
71. SCHAFE, G. E. et al. Memory consolidation for contextual and auditory fear conditioning is dependent on protein synthesis, PKA, and MAP kinase. *Learning & Memory*, v. 6, n. 2, p. 97–110, 1 mar. 1999.
72. BARSEGYAN, A. et al. Glucocorticoids in the prefrontal cortex enhance memory consolidation and impair working memory by a common neural mechanism. *Proceedings of the National Academy of Sciences*, v. 107, n. 38, p. 16655–16660, 21 set. 2010.
73. SILVA, T. R.; DIAS, F. A. M. Diferenças na habilidade de integração auditiva inter-hemisférica entre os gêneros feminino e masculino: estudo preliminar. *Revista da Sociedade Brasileira de Fonoaudiologia*, v. 17, n. 3, p. 260–265, 2012.
74. MACHADO, A. P. R.; CARVALHO, I. O.; ROCHA SOBRINHO, H. M. da. Neuroinflamação na Doença de Alzheimer. *Revista Brasileira Militar de Ciências*, v. 6, n. 14, 3 fev. 2020.
75. SALIM, P. H.; XAVIER, R. M. Influência dos polimorfismos genéticos (IL10/CXCL8/CXCR2/NFκB) na susceptibilidade das doenças reumatológicas autoimunes. *Revista Brasileira de Reumatologia*, v. 54, n. 4, p. 301–310, jul. 2014.
76. ABOZAID, O. A. R. et al. Resveratrol-selenium nanoparticles alleviate neuroinflammation and neurotoxicity in a rat model of Alzheimer's disease by regulating Sirt1/miRNA-134/GSK3β expression. *Biological Trace Element Research*, v. 200, n. 12, p. 5104–5114, 21 dez. 2022.
77. TOSI, G.; DUSKEY, J. T.; KREUTER, J. Nanoparticles as carriers for drug delivery of macromolecules across the blood-brain barrier. *Expert Opinion on Drug Delivery*, v. 17, n. 1, p. 23–32, jan. 2020.